Biocontrol Science, 2018, Vol. 23, No. 2, 61－69

Original

Comparison of the Filter Efficiency of Medical Nonwoven Fabrics against Three Different Microbe Aerosols

NORIKO SHIMASAKI[1]*, AKIRA OKAUE[2], RITSUKO KIKUNO[2], AND KATSUAKI SHINOHARA[1]

[1]*National Institute of Infectious Diseases, 4-7-1 Gakuen, Musashimurayama-shi, Tokyo, Japan*
[2]*Kitasato Research Center for Environmental Science, 1-15-1 Kitasato, Minami, Sagamihara, Kanagawa, Japan*

Received 24 June, 2017/Accepted 18 October, 2017

Exact evaluation of the performance of surgical masks and biohazard protective clothing materials against pathogens is important because it can provide helpful information that healthcare workers can use to select suitable materials to reduce infection risk. Currently, to evaluate the protective performance of nonwoven fabrics used in surgical masks against viral aerosols, a non-standardized test method using phi-X174 phage aerosols is widely performed because actual respiratory viruses pose an infection risk during testing and the phage is a safe virus to humans. This method of using a phage is simply modified from a standard method for evaluation of filter performance against bacterial aerosols using *Staphylococcus aureus*, which is larger than virus particles. However, it is necessary to perform such evaluations based on the size of the actual pathogen particles. Thus, we developed a new method that can be performed safely using inactivated viral particles and can quantitate the influenza virus in aerosols by antigen-capture ELISA (Shimasaki et al., 2016a). In this study, we used three different microbial aerosols of phi-X174 phage, influenza virus, and *S. aureus* and tested the filter efficiency by capturing microbial aerosols for two medical nonwoven fabrics. We compared the filter efficiency against each airborne microbe to analyze the dependency of filter efficiency on the microbial particle size. Our results showed that against the three types of spherical microbe particles, the filter efficiencies against influenza virus particles were the lowest and those against phi-X174 phages were the highest for both types of nonwoven fabrics. The experimental results mostly corresponded with theoretical calculations. We conclude that the filter efficiency test using the phi-X174 phage aerosol may overestimate the protective performance of nonwoven fabrics with filter structure compared to that against real pathogens such as the influenza virus.

Key words：Aerosol / Filter efficiency / Influenza virus / Phi-X174 phage / *Staphylococcus aureus*.

INTRODUCTION

Influenza is a respiratory disease of which outbreaks are seen worldwide every year. Many cases of nosocomial infections involving the influenza virus have also been reported (Álvarez-Lerma et al., 2017; Dare and Talbot, 2016; Hagel et al., 2016), and healthcare workers must use suitable biohazard protective clothing and equipment to reduce infection risks (Kaye et al., 2015). Among the available protective clothing and equipment, surgical masks are frequently used as a standard precaution because the infection route of influenza involves the upper respiratory tract such as the throat or nasal passages. Therefore, it is important to exactly evaluate the performance of the surgical mask materials against pathogens.

Currently, there is no standard method for evaluating the protective performance of nonwoven fabrics used in surgical masks against viral aerosols, although there are standard methods for testing fabrics against bacterial aerosols using *Staphylococcus aureus* (ASTM F2100-11, 2011; JIS L 1912, 1997), which is larger than virus particles. However, a test method modified to use a

**Corresponding author. Tel: +81-42-561-0771, Fax: +81-42-561-6156, E-mail : shima(a)nih.go.jp*

phi-X174 phage aerosol as a safe model virus is widely performed (https://www.nelsonlabs.com/Test/Viral-Filtration-Efficiency, accessed on May 15, 2017) because tests using actual respiratory viruses are associated with a risk of infection during testing.

In a model aerosol study, Turgeon et al. (2014) compared the effects of aerosolization and sampling on the infectivity of five tail-less bacteriophages and two pathogenic viruses. They concluded that the behavior of the influenza virus resembled those of the PR772 and Φ6 phages, whereas the behavior of the Newcastle disease virus was more similar to those of the MS2 and ΦX174 phages. However, they only examined the initial ratio between the number of viable particles and the amount of nucleic acids in the aerosol using a culture assay and quantitative PCR, and did not investigate how easily the viral aerosol could pass through the nonwoven filter used for surgical masks.

We consider that it is necessary to perform these evaluations based on the size of real pathogen particles, especially that of the influenza virus because its small particle diameter (approximately 0.1 μm) might enable it to easily pass through nonwoven filters, as evidenced by previous studies on the penetration of nanoparticles (not viral particles) through surgical masks (Huang et al., 1998; Lee et al., 2008). Thus, we developed a new method that can be used to safely perform tests by using an inactivated influenza virus (inact-IFV) and quantitating viral aerosols with antigen-capture ELISA (Shimasaki et al., 2016a).

In this study, tests of the filter efficiency of nonwoven fabrics for medical use to capture virus particles in aerosols were performed by individually using phi-X174 phage aerosols and influenza virus aerosols, and we compared their filter efficiency. In addition, the filter efficiency against *S. aureus*, which has a larger particle size than the influenza virus and is used in the JIS test (JIS L 1912, 1997), was also tested to investigate the dependence of the filter efficiency on microbial particle size. The respective particle size of the microbes in the test microbe suspension was characterized before the aerosol test. Furthermore, the filter efficiency depending on microbial particle size was analyzed based on the theoretical calculation for physical aerosol technology.

MATERIALS AND METHODS

Preparation of the phi-X174 phage

The phi-X174 phage (ATCC 13706-B1) was prepared as described in a previous study (Shimasaki et al., 2016b). The stock phi-X174 phage (approximately 1×10^{10} plaque-forming units (PFU)/mL) was distilled 50-fold with distilled water (DW) as a test phi-X174 phage suspension, which contained 1.8×10^{8} PFU/mL.

Quantitative measurement of the phi-X174 phage

The phage titer was determined by a soft-agar-overlaid plaque assay, as previously described (Shimasaki et al., 2016b). Briefly, the assay fluid was 10-fold serially diluted with PBS, and 0.2 mL of each serial dilution or undiluted assay fluid mixed with 0.2 mL of the host *E. coli* (ca. 10^{9} colony-forming units [CFU]/mL) was added to tubes containing 4 mL of nutrient broth with 0.5% NaCl and 0.5% agar. After gentle mixing, the suspension was poured onto two plates of nutrient agar. After cultivation for 18 h at 37℃, the plaques on the plates were counted.

Preparation of *S. aureus*

S. aureus (NBRC 12732) was prepared as described in a previous study (Shimasaki et al., 2016b), with modification. *S. aureus* was cultured on tryptic soy agar (TSA; Difco, Becton, Dickinson and Company) for 24 h at 35℃. The colonies on the agar plate were suspended in DW at a concentration of 2-5×10^{8} CFU/mL. The test suspension of *S. aureus* contained 3.3×10^{8} CFU/mL.

Quantitative measurement of *S. aureus*

The amount of *S. aureus* was determined by culture assay as described in a previous study (Shimasaki et al., 2016b). Briefly, 100 μL of the assay fluid was 10-fold serially diluted with PBS, and each serial dilution or undiluted assay fluid was spread onto two TSA plates. The plates were cultured for 48 h at 35℃, and the number of colonies was then counted.

Preparation of inact-IFV

The inact-IFV was prepared as described in a previous study (Shimasaki et al., 2016a). The test suspension of inact-IFV was diluted to a total protein content of ca. 120 μg/mL with Dulbecco's phosphate-buffered saline (DPBS) before use. The M1 protein concentration of the test virus suspension was 89 μg/mL, as determined by ELISA.

Quantitative measurement of inact-IFV

The amount of inact-IFV was determined with antigen-capture ELISA as described in a previous study (Shimasaki et al., 2016a). Briefly, the wells of a microplate were coated with 100 μL of antigen-capturing monoclonal antibody 29D2 (0.2 mg/mL) in carbonate-bicarbonate buffer and incubated at 4℃ overnight. After being washed with Tris-buffered saline containing 0.1% Tween20 (TBS-T), the microplate was blocked with 300 μL of blocking buffer at room temperature for 1.5-2 h. After being washed with TBS-T, the microplate was reacted with serial dilutions (DPBS containing 0.02% gelatin and 0.1% Triton X-100; gelaDPBS-TX) of the PR8 virus or M1 protein standard (recombinant H1N1

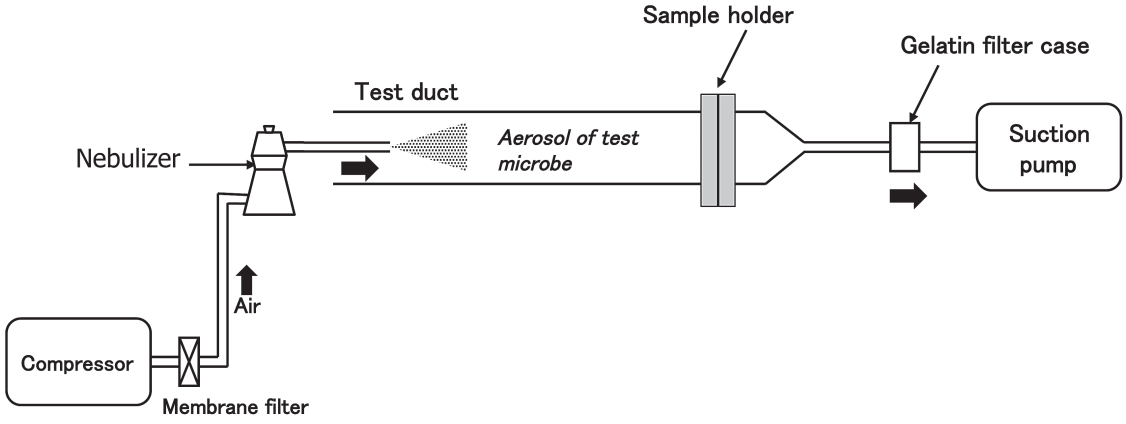

FIG. 1. Setup of the test device.
The nebulizer was fitted upstream of the airflow in the test duct, which contained the sample holder. The nonwoven material to be tested was held in the sample holder. The test microbe suspension was placed in the nebulizer. A gelatin filter with a dedicated filter case was connected to the test duct, downstream of the airflow. Air from a compressor was fed into the nebulizer at 3 L/min to spray the test microbe aerosol into the test duct. At the same time, a suction pump was actuated at 5 L/min for 3 min (15 L in total) to collect on the gelatin filter the test microbe aerosol that penetrated through the test materials. The test was performed three times at 20-23℃ and 20-40% relative humidity.

[A/Puerto Rico/8/34/Mount Sinai] M1 protein) at 37℃ for 1.5 h. After washing with TBS-T, 100 µL of anti-flu A M1 goat polyclonal antibody was added to the wells, and the plate was incubated at 37℃ for 1 h. After washing with TBS-T, 100 µL of anti-goat IgG-HRP was added to the wells, and the plate was incubated at 37℃ for 1 h. The plate was then washed with TBS-T, and 100 µL of TMB-substrate was added. The reaction was stopped by adding 100 µL of TMB Stop Buffer, and the optical density at 450 nm was measured using a multi-well plate reader.

Dynamic light scattering (DSL)

The particle size distribution of the test microbe suspension was determined by DLS as described in a previous study (Shimasaki et al., 2016a). The suspension was measured for 10 s at room temperature in a Viscotek Model 802 DLS system with Omni Size 3.0 (Viscotek, Texas, USA).

Transmission electron microscopy (TEM)

TEM images were obtained as described in a previous study (Shimasaki et al., 2016a). The test virus suspension was negatively stained with 2% phosphotungstic acid on a 400-mesh copper grid coated with carbon. Images were obtained using a JEM-1400 transmission electron microscope (JEOL Ltd., Tokyo, Japan) operated at 80 kV.

Scanning electron microscopy (SEM)

SEM images were prepared at Japan Microbiological Clinic Co., Ltd. (Kanagawa, Japan).

Test nonwoven fabrics

Two types of nonwoven fabrics used in commercially available surgical masks and protective clothing were selected for this study: nonwoven fabric samples 1 (Spunbond/Meltblown/Spunbond[SMS]-type) and 2 (Spunlace-type), which are categorized as different types of nonwoven fabric structure (Shinohara and Shimasaki, 2012). The different structures of nonwoven fabric were derived from different manufacturing processes. SMS has three bonded layers, Spunbond/Meltblown/Spunbond, and Spunlace has a structure in which fibers are intertwined by a high-pressure water stream into a mono-layer (Yaida, 1995). A surface image of sample 2 was obtained using a stereoscopic microscope (Model SZH ILLC2, Olympus Co., Tokyo, Japan). The thickness of the fabric samples was determined as an average value, excluding the maximum and minimum values, of seven points measured with an SM-114 dial thickness gage (Teclock Co., Nagano, Japan).

Filter performance test against the three individual aerosols

Three individual aerosols, each containing one of the microbes, were prepared. The test devices were set up in a biosafety cabinet (Fig.1), as described in a previous study (Shimasaki et al., 2016a). The nebulizer (a custom-made glass or NE-C16, Omron Healthcare Co., Ltd., Kyoto, Japan) was fitted upstream of the airflow in the test duct, which contained the sample holder. The sample fabric was held in place in the sample holder. The test microbe suspension was placed

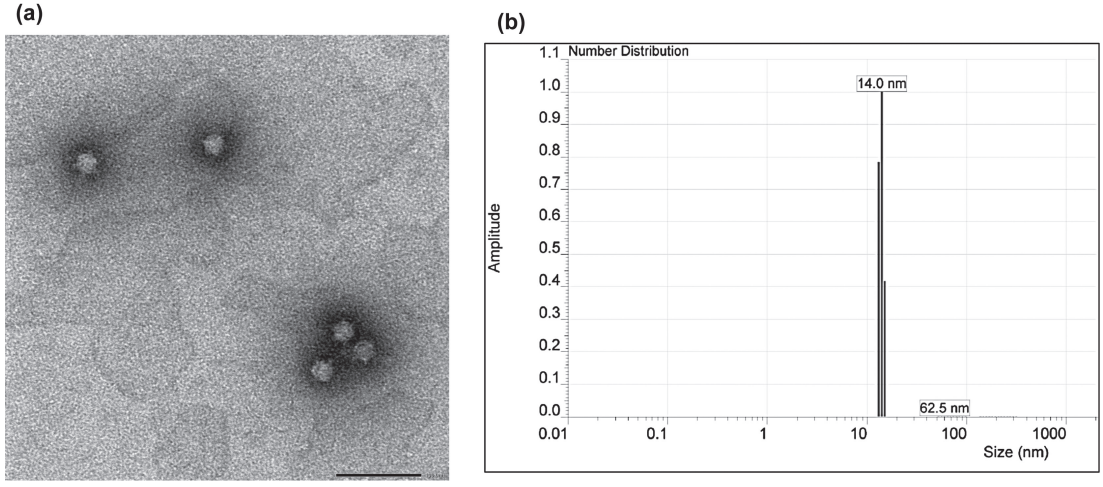

FIG. 2. Characterization of the phi-X174 phage.
(a) Negatively stained Transmission electron microscopy (TEM) image; scale bar,100 nm. (b) Dynamic light scattering (DLS) analysis of the phi-X174 phage in the test suspension. Particle size distribution of the phi-X174 phage in the test suspension was estimated by DLS. The size on the horizontal axis indicates the hydrodynamic radius (Rh).

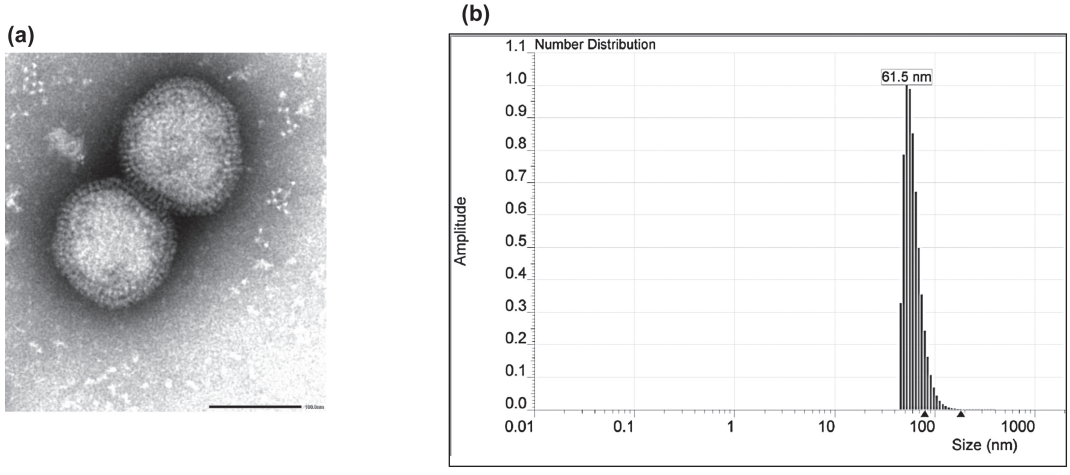

FIG. 3. Characterization of inact-IFV.
(a) Negatively stained TEM image; scale bar is 100 nm. (b) DLS analysis of inact-IFV in the test suspension. Particle size distribution of inact-IFV in the test suspension was estimated by DLS.

in the nebulizer, and a gelatin filter (12602-47-ALK; Sartorius, Gottingen, Germany) with a dedicated filter case was connected to the test duct, downstream of the airflow.

Air from a compressor was fed into the nebulizer at an airflow rate of 3 L/min to spray the inactivated influenza virus aerosol into the test duct. At the same time, a suction pump was actuated at an airflow rate of 5 L/min for 3 min (15 L in total) to collect on the gelatin filter the test microbe aerosol that penetrated through the test materials. The velocity of the passing aerosol was calculated to be 4.24 cm/s. The test was performed three times at 20-23℃ and 20-40% relative humidity.

To determine the amount of microbial aerosol that penetrated the test material, the gelatin filter was dissolved in 5 mL of DPBS at 37℃, and the amount of test microbe in this dissolved solution was assayed. For inact-IFV, DPBS containing 0.02% gelatin and 0.1% Triton X-100 (9 volumes) was added to the gelatin filter suspension before the assay.

RESULTS

Characterization of the test microbe suspension

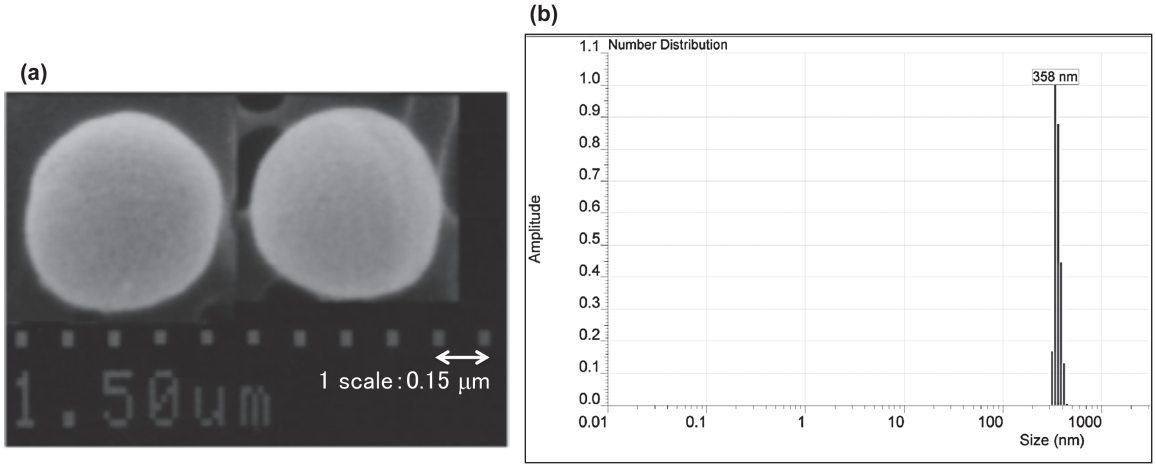

FIG. 4. Characterization of *S. aureus*.
(a) Scanning electron microscopy (SEM) image of *S. aureus*; scale bar is 0.15 μm. (b) DLS analysis of *S. aureus* in the test suspension. Particle size distribution of *S. aureus* in the test suspension was estimated by DLS.

TEM analysis of the phi-X174 phage and inact-IFV and SEM analysis of *S. aureus* revealed that the virus particles were almost spherical in shape. The diameter of the phage particles was 25-30 nm (Fig.2(a)), the diameter of inact-IFV was 120-130 nm (Fig.3(a)), and the diameter of *S. aureus* was 0.6-0.7 μm (Fig.4(a)). To confirm the size of the test microbe particles in the suspension and to determine whether any aggregation of the test microbe particles had occurred, we investigated the characteristics of the test microbes using DLS. The particle size distribution of the phi-X174 phage in the test suspension expressed in terms of the hydrodynamic radius (Rh) revealed a peak at 14.0 nm and a negligible peak at 62.5 nm (Fig.2(b)). The particle size of the inact-IFV was 61.5 nm (Fig.3(b)), and that of *S. aureus* was 358 nm (Fig.4(b)). Using the Rh value, the diameters of the particles in the test microbe suspension were estimated to be approximately 28 nm for phi-X174, 120 nm for inact-IFV, and 0.7 μm for *S. aureus*, which were equivalent to those determined by TEM or SEM analysis. In addition, one sharp peak in the particle distribution was observed in each test suspension. These results indicate that the particles of each test microbe were monodisperse.

Filter performance test of the medical nonwoven fabrics against the three test microbe aerosols

We tested the filter performance of the two test nonwoven fabrics against the three test microbe aerosols (Table 1). The amount of the test microbe in each aerosol that penetrated through the test fabrics or without test materials (no filter) were determined by culture assay or ELISA.

Figure 5 shows the penetration ratios of the three different microbe aerosols for each sample. The penetration ratio was calculated using the following equation: penetration ratio (%) = (test microbe amount for each sample)/(test microbe amount for the blank experiment [no filter]). For sample 1 and sample 2, the penetration ratio of influenza virus particles was the highest, and that of the phi-X174 phage was the lowest. The penetration ratios for sample 1 were also significantly different between phi-X-174 and inact-IFV (t-test: $P < 0.001$). The penetration ratios for sample 2 were significantly different between phi-X-174 and inact-IFV (t-test: $P < 0.001$), between phi-X-174 and *S. aureus* (t-test: $P < 0.05$), and between inact-IFV and *S. aureus* (t-test: $P < 0.05$). As the filter efficiency was calculated as 100% - the penetration ratio, the filter efficiency against influenza virus particles (particle diameter of approximately 120 nm determined by DLS) was the lowest, and that against the phi-X174 phage (approximately 28 nm) was the highest among the three types of spherical microbe particles.

Theoretical calculation of the filter efficiency against the three different microbe aerosols

Finally, the filter efficiency against the three different microbe aerosols was analyzed based on aerosol technology and compared to the experimental results. The filter efficiency = 1 – the penetration ratio.

The penetration ratio (R_p) for the fiber layer filter can be estimated from the collection efficiency of one fiber (η_Σ) (Eq.1, 2, 3, 4, 5, and 6) (Hinds, 1999; Otani and Seto, 2009). The following parameters were used: η_R, η_I, η_G, and η_D are the single-fiber efficiency for interception, impaction, gravitational setting, and diffusion, respectively. d_p is the size of the particle to be

TABLE 1. Filter performance of nonwoven fabrics against the three test microbe aerosols.

	Phi-X174 phage amount (PFU/sampling)			
Experimental condition	1st	2nd	3rd	Ave.
Sample 1	3.2×10^4	3.8×10^4	3.5×10^4	3.5×10^4
Sample 2	1.4×10^5	1.8×10^5	1.7×10^5	1.6×10^5
Blank (no filter)	7.5×10^5	3.0×10^5	6.2×10^5	5.6×10^5
	Inact-IFV amount (ngM1/sampling)			
Experimental condition	1st	2nd	3rd	Ave.
Sample 1	4.67×10^2	3.50×10^2	4.38×10^2	4.18×10^2
Sample 2	1.82×10^3	1.60×10^3	1.90×10^3	1.78×10^3
Blank (no filter)	1.94×10^3	2.66×10^3	2.11×10^3	2.24×10^3
	S. aureus amount (CFU/sampling)			
Experimental condition	1st	2nd	3rd	Ave.
Sample 1	5.4×10^5	1.4×10^6	1.0×10^6	9.8×10^5
Sample 2	3.8×10^6	5.6×10^6	4.4×10^6	4.6×10^6
Blank (no filter)	6.2×10^6	8.6×10^6	1.0×10^7	8.3×10^6

Filter performance tests for the test materials (samples 1 and 2 to blank) against the three test microbes in the aerosol were performed. The amounts of the test microbe aerosol per sampling are shown. Tests were performed three times on each experimental condition and the average (Ave.) was determined.

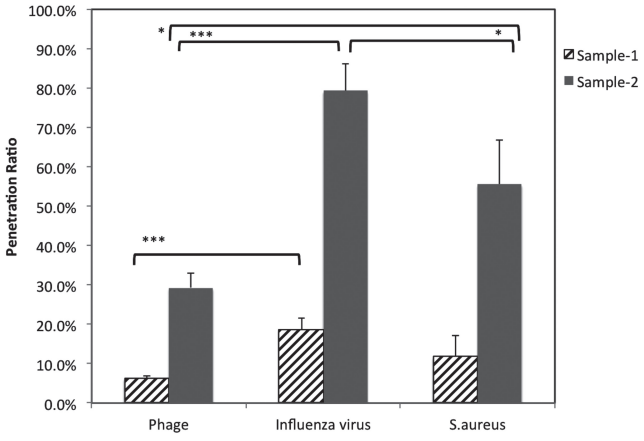

FIG. 5. Comparison of the penetration ratios of the three different microbe aerosols.
The penetration ratio of each airborne microbe for the test materials (samples 1, 2) was calculated based on the amount of the test microbe aerosol shown in Table 1: penetration ratio (%) = (test microbe amount for each sample)/(test microbe amount for the blank experiment [no filter]). Average values of penetration ratios are shown. Error bars denote the standard deviation.
$^*P < 0.05$, $^{***}P < 0.001$ by t-test.

collected, D is the particle diffusion coefficient, C_c is the Cunningham correction factor, d_f is the fiber diameter, α is the filling rate of the fiber, t is the filter thickness, U is the velocity of the passing aerosol, and μ is the viscosity of the air (1.81×10^{-5} Pa·s).

$$R_p = \exp\left(\frac{-4\alpha\eta_\Sigma t}{\pi d_f(1-\alpha)}\right) \quad \cdots \text{(Eq.1)}$$

$$\eta_\Sigma = \eta_R + \eta_I + \eta_G + \eta_D \quad \cdots \text{(Eq.2)}$$

$$\eta_R = \frac{(1-\alpha)R^2}{Ku(1+R)} \quad \cdots \text{(Eq.3)}$$

where $R = \frac{d_p}{d_f}$, $Ku = -\frac{\ln\alpha}{2} - \frac{3}{4} + \alpha - \frac{\alpha^2}{4}$

$$\eta_I = \frac{(Stk)J}{2Ku^2} \quad \cdots \text{(Eq.4)}$$

where $Stk = \frac{\rho_p d_p^2 C_c U}{18\mu d_f}$,

and ρ_p is particle density (1 g/cm^3),

in case of $d_p > 0.1$ μm, $C_c = 1 + 2.52\,\lambda/d_p$,

in case of $d_p \leqq 0.1$ μm,

$$C_C = 1 + \frac{\lambda}{d_p}\left[2.414 + 0.880\exp\left(-0.39\frac{d_p}{\lambda}\right)\right],$$

λ is the mean free path (0.064 μm),

$J = (29.6 - 28\alpha^{0.62})R^2 - 27.5R^{2.8}$

$$\eta_G = 2.7Pe^{-2/3} \quad \cdots \text{(Eq.5)}$$

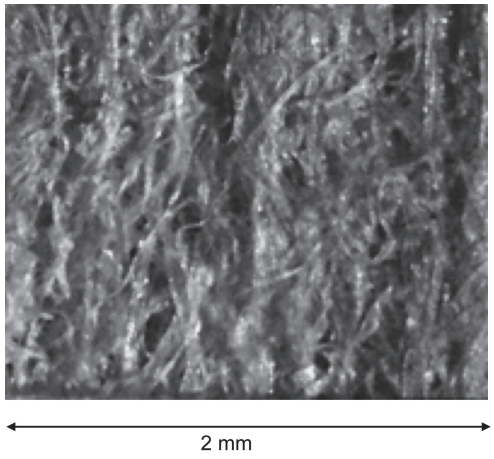

FIG. 6. Surface image of sample 2.
The surface of sample 2 was observed with a microscope. The fiber diameter of sample 2 was 17 μm.
Scale bar is 2 mm.

where $Pe = \frac{d_f U}{D}$, $D = \frac{C_c kT}{3\pi\mu d_p}$,

k is Boltzmann's constant, and T is absolute temperature (293 K)

$$\eta_G = G(1+R) \quad \cdots \text{(Eq.6)}$$

where $G = \frac{\rho_g d_p^2 C_c g}{18\mu U}$,

and ρ_g is air density (1.2 kg/m^3)

We calculated the penetration ratio according to particle size ranging from 0.01 μm to 5 μm for sample 2, as shown in Figure 7 with arrows indicating the particle sizes of the three microbes determined by DLS, using the following parameter values:

d_f = 17 μm by observation of the filter surface (Fig.6),
t = 0.284 mm by measurement
α = 0.25 by calculation of the filter weight (70.4 g/m^2) divided by t assuming that the fiber density is 1 g/cm^3.
U = 4.24 cm/s (Materials and Methods)

Our analysis showed that the calculated penetration ratio of the phi-X174 phage was the lowest of the three microbes. This means that the calculated filter efficiency against the phi-X174 phage was the highest among those against the three microbes. The calculated penetration ratio of inact-IFV was the higher, and the calculated filter efficiency against inact-IFV was the lower than the phage. The experimental penetration ratios obtained using each test microbe, i.e., the phi-X174 phage and inact-IFV, mostly corresponded with this calculation. However, the experimental results for *S. aureus* did not agree with our calculation.

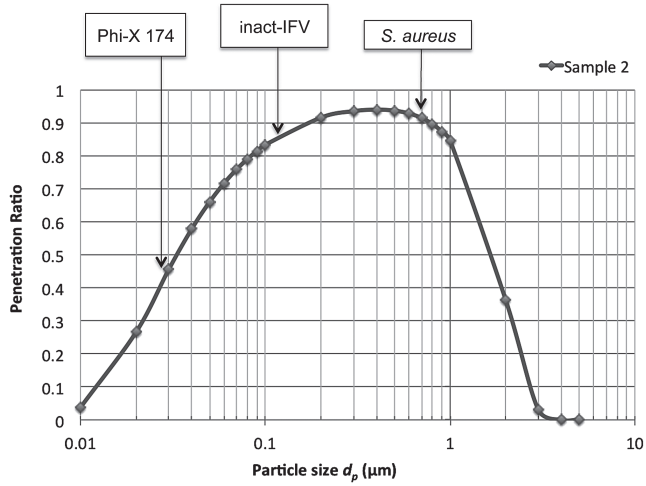

FIG. 7. Theoretical calculations of the penetration ratio according to particle size.
The theoretically calculated penetration ratio of the phi-X174 phage was the lowest among the three microbes, and that of inact-IFV was the higher than the phage. The experimental penetration ratios for the phi-X174 phage and inact-IFV roughly agreed with this calculation.

DISCUSSION

In this study, we compared the filter efficiencies of medical nonwoven fabrics using aerosols containing three test microbes: the phi-X174 phage, influenza virus, and *S. aureus*. Among the three types of spherical microbe particles, the filter efficiency against influenza virus particles (particle diameter of approximately 120 nm determined by DLS) was the lowest, and that against the phi-X174 phage (approximately 28 nm) was the highest for both sample 1 and 2. These findings suggest that the result of filter efficiency tests using the phi-X174 phage could be overestimated, compared with the filter efficiency against real pathogens such as the influenza virus. When the filter efficiency against pathogens with almost the same size particle as that of the phi-X174 phage, e.g., norovirus or hepatitis A virus, is evaluated, the filter efficiency test using the phi-X174 phage may be sufficient. Incidentally, we speculate that sample 1 had a lower penetration ratio against all microbe particles compared with sample 2, because sample 1 has a three-layered structure (SMS-type), different from sample 2. If theoretical calculations could be also made for sample 1, it might be possible to explain in detail the mechanism that causes the difference in the penetration ratio between samples 1 and 2. However, it is difficult to determine α (the filling rate of the fiber) and d_f (the fiber diameter) required for theo-

retical calculations of the penetration ratio in the case of a three-layered structure such as that in sample 1. Further studies may be needed.

Our results indicate that filter efficiency tests with the inactivated influenza virus would provide information that better reflects a material's capacity for protection against a real airborne pathogen. This study also aimed to clarify the usefulness of the ELISA we developed for evaluating the filter efficiency against the influenza virus aerosol because the inactivated influenza virus is as safe for use in performance testing as the phi-X174 phage.

A previous report tested the filter efficiency of several respiratory protection devices, two types of N95 masks and two types of surgical masks using the MS2 virus (Bałazy et al., 2006). It was found that the penetration rate of aerosol particles containing the MS2 phage through the surgical mask increased as the particle size increased from 10 nm to 80 nm, which is consistent with our results ranging from 28 nm to 120 nm. Rengasamy et al. (2017) compared facemask and respirator filtration test methods and concluded that the higher efficiencies obtained using viral filtration efficiency test methods with phi-X174 demonstrate that addition of these supplemental particle penetration methods will not improve respirator certification, which agrees with our conclusion.

This study has some limitations. Our calculated analysis (Fig.7) could not explain the experimental results for the *S. aureus* aerosol. Although this calculated analysis did not consider the influence of the electrical surface charge of *S. aureus* particles, further studies for accurate prediction are needed. Moreover, other viruses that cause serious respiratory diseases worldwide should also be considered. For example, outbreaks of measles (Davoodian et al., 2017, Mollema et al., 2015) and Middle East respiratory syndrome coronavirus (MERS-Cov) (Guery et al., 2013) have been reported recently. The particle size of the MERS-Cov is approximately 100 nm (http://www.niid.go.jp/niid/ja/iasr-sp/2320-related-articles/related-articles-430/6116-dj4304.html, accessed on May 26, 2017) and that of the measles virus is 100-250 nm (https://www.niid.go.jp/niid/ja/kansennohanashi/518-measles.html, accessed on May 26, 2017). In addition to the influenza virus used in this study, other viruses should be studied in the future.

Our results revealed that the filter efficiency test using the phi-X174 phage aerosol will possibly overestimate the protective performance of medical nonwoven fabrics compared to that against real pathogens such as the influenza virus. The results of our study should help healthcare workers when selecting appropriate masks and protective clothing, depending on the hazardous situation and infection risk.

ACKNOWLEDGMENT

We would like to thank Prof. S. Kato at the Institute of Industrial Science of the University of Tokyo for providing helpful advice.

REFERENCES

Álvarez-Lerma, F., Marín-Corral, J., Vilà, C., Masclans, J. R., Loeches, I. M., Barbadillo, S., González, de Molina, F. J., and Rodríguez, A. H1N1 GETGAG/SEMICYUC Study Group. (2017) Characteristics of patients with hospital-acquired influenza A (H1N1)pdm09 virus admitted to the intensive care unit. *J. Hosp. Infect*., **95**, 200-206.

ASTM F2100-11 (2011) Standard Specification for Performance of Materials Used in Medical Face Masks. *ASTM International*.

Bałazy, A., Toivola, M., Adhikari, A., Sivasubramani, S. K., Reponen, T., and Grinshpun, S. A. (2006) Do N95 respirators provide 95% protection level against airborne viruses, and how adequate are surgical masks? *Am. J. Infect. Control*, **34**, 51-57.

Dare, R. K., and Talbot, T. R. (2016) Health Care-Acquired Viral Respiratory Diseases. *Infect. Dis. Clin. North. Am*., **30**, 1053-1070.

Davoodian, P., Atashabparvar, A., Dadvand, H., Hosseinpour, M., Daryanavard, A., Safari, R., Rastegar, A., Khajeh, E., and Mahboobi, H. (2017) A report of outbreaks of measles on the southern coast of Iran from 2009 to 2015. *Electron. Physician*, **9**, 3997-4002.

Guery, B., Poissy, J., el Mansouf, L., Séjourné, C., Ettahar, N., Lemaire, X., Vuotto, F., Goffard, A., Behillil, S., Enouf, V., Caro, V., Mailles, A., Che, D., Manuguerra, J. C., Mathieu, D., Fontanet, A., van der Werf, S., and MERS-CoV study group. (2013) Clinical features and viral diagnosis of two cases of infection with Middle East Respiratory Syndrome coronavirus: a report of nosocomial transmission. *Lancet*, **381**, 2265-2272.

Hagel, S., Ludewig, K., Moeser, A., Baier, M., Löffler, B., Schleenvoigt, B., Forstner, C., and Pletz, M. W. (2016) Characteristics and management of patients with influenza in a German hospital during the 2014/2015 influenza season. *Infection*, **44**, 667-672.

Hinds, W. C. (1999) Aerosol Technology, Second Edition, John Wiley & Sons Inc., pp49, 183-205.

Huang, C., Willeke, K., Qian, Y., Grinshpun, S., and Ulevicius, V. (1998) Method for measuring the spatial variability of aerosol penetration through respirator filters. *Am. Ind. Hyg. Assoc. J*., **59**, 461-465.

JIS L 1912 (1997) Test methods for nonwoven fabrics of medical use (in Japanese). *Japanese Industrial Standards*.

Kaye, K. S., Anderson, D. J., Cook, E., Huang, S. S., Siegel, J. D., Zuckerman, J. M., and Talbot, T. R. (2015) Guidance for infection prevention and healthcare epidemiology programs: healthcare epidemiologist skills and competencies. *Infect. Control Hosp. Epidemiol*., **36**, 369-380.

Lee, S. A., Grinshpun, S. A., and Reponen, T. (2008) Respiratory performance offered by N95 respirators and surgical masks: human subject evaluation with NaCl aerosol representing bacterial and viral particle size range. *Ann. Occup. Hyg*., **52**, 177-185.

Mollema, L., Harmsen, I. A., Broekhuizen, E., Clijnk, R., De Melker, H., Paulussen, T., Kok, G., Ruiter, R., and Das, E. (2015) Disease Detection or Public Opinion Reflection? Content Analysis of Tweets, Other Social Media, and Online Newspapers During the Measles Outbreak in the Netherlands in 2013. *J. Med. Internet. Res*., **17**, e128.

Otani, Y., and Seto, A. (2009) Kougyou Nano Ryushi no Filter seinou shiken ni Kansuru Tejunsho (in Japanese). https://www.aist-riss.jp/projects/nedo-nanorisk/nano_rad2/docs/preparation/nano_filter-prep.pdf. p31-32. Accessed on 2017.4.3.

Rengasamy, S., Shaffer, R., Williams, B., and Smit, S. (2017) A comparison of facemask and respirator filtration test methods. *J. Occup. Environ. Hyg*., **14**, 92-103.

Shimasaki, N., Hara, M., Kikuno, R., and Shinohara, K. (2016b) A highly sensitive assay using synthetic blood containing test microbes for evaluation of the penetration resistance of protective clothing material under applied pressure. *Biocontrol Sci*., **21**, 141-152.

Shimasaki, N., Nojima, Y., Okaue, A., Takahashi, H., Kageyama, T., Hamamoto, I., and Shinohara, K. (2016a) A Novel Method of Safely Measuring Influenza Virus Aerosol Using Antigen-Capture Enzyme-Linked Immunosorbent Assay for the Performance Evaluation of Protective Clothing Materials. *Biocontrol Sci*., **21**, 81-89.

Shinohara, K., and Shimasaki, N. (2012) Performance evaluation of protective clothing materials for biohazard measures (in Japanese). *Clean technology*, **22**, 58-64.

Turgeon, N., Toulouse, M. J., Martel, B., Moineau, S., and Duchaine, C. (2014) Comparison of five bacteriophages as models for viral aerosol studies. *Appl. Environ. Microbiol*., **80**, 4242-4250.

Yaida, O. (1995) Saikin no Hushokuhu no Doukou (in Japanese). *SEN-I GAKKAISHI*, **51**, 200-205.